

TTCBF: A Truncated Taylor Control Barrier Function for High-Order Safety Constraints [★]

Jianye Xu ^a, Bassam Alrifaee ^b,

^a*Chair of Embedded Software, RWTH Aachen University, Aachen 52072, Germany*

^b*Department of Aerospace Engineering, University of the Bundeswehr Munich, Munich 85579, Germany*

Abstract

Control Barrier Functions (CBFs) enforce safety by rendering a prescribed safe set forward invariant. However, standard CBFs are limited to safety constraints with relative degree one, while High-Order CBF (HOCBF) methods address higher relative degree at the cost of introducing a chain of auxiliary functions and multiple class \mathcal{K} functions whose tuning scales with the relative degree. In this paper, we introduce a Truncated Taylor Control Barrier Function (TTCBF), which generalizes standard discrete-time CBFs to consider high-order safety constraints and requires only one class \mathcal{K} function, independent of the relative degree. We also propose an adaptive variant, adaptive TTCBF (aTTCBF), that optimizes an online gain on the class \mathcal{K} function to improve adaptability, while requiring fewer control design parameters than existing adaptive HOCBF variants. Numerical experiments in a relative-degree-six spring-mass system and a cluttered corridor navigation validate the above theoretical findings.

Key words: Control barrier function; Lyapunov methods; Optimal control; Safety-critical control.

1 Introduction

Control Barrier Functions (CBFs) are a standard tool for safety-critical control, where safety is specified as forward invariance of a set defined by a barrier inequality [3]. In the CBF framework, one encodes a state constraint through a continuously differentiable function and derives a pointwise inequality constraint on the control input whose satisfaction implies forward invariance of the safe set. When combined with a Control Lyapunov Function (CLF) constraint and a quadratic objective, this construction yields a sequence of Quadratic Programs (QPs) that can be solved online, giving rise to the widely used CLF-CBF-QP framework [4,8]. This framework has been demonstrated in applications such as autonomous driving [4,20] and safe navigation for mobile robots [6,19], where it provides real-time implementability together with closed-loop safety guarantees.

Class \mathcal{K} functions play a central role in CBFs because they regulate how the barrier value evolves as the state

[★] This paper was not presented at any IFAC meeting. Corresponding author J. Xu. Tel. +49 241 80-21149. Fax +49 241 80-22150.

Email addresses: xu@embedded.rwth-aachen.de (Jianye Xu), bassam.alrifae@unibw.de (Bassam Alrifae).

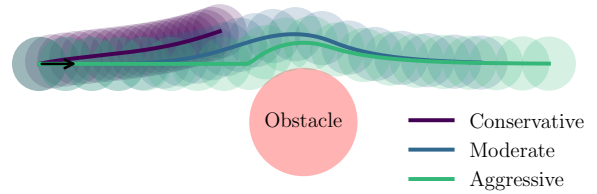


Fig. 1. An obstacle-avoidance example with three different parameters of a class \mathcal{K} function: conservative, moderate, and aggressive. Footprints: circles; trajectories: solid lines.

approaches the safety boundary. Their parameters directly affect the trade-off between conservatism and aggressiveness: conservative choices can shrink the feasible set of the associated QP and lead to infeasibility under tight control bounds [10], whereas aggressive choices can allow rapid motion toward the boundary and increase the likelihood of infeasibility when the state reaches the boundary. Fig. 1 illustrates how this tuning changes the resulting obstacle-avoidance behavior, ranging from slow and conservative to fast and aggressive maneuvers.

A further limitation of standard CBFs is their reliance on relative-degree-one constraints. The relative degree of a

safety constraint with respect to a system is the number of times one needs to differentiate it along the system dynamics before the control input appears explicitly. For higher-relative-degree constraints, early approaches include backstepping-based constructions [9] and exponential CBFs based on input–output linearization [14]. The High-Order CBF (HOCBF) in [16] provides a constructive extension that handles arbitrarily high relative degree by introducing a chain of auxiliary functions. This construction uses one class \mathcal{K} function at each level of the chain, so the number of class \mathcal{K} functions, and hence the number of associated tuning parameters, grows with the relative degree. Several methods aim to reduce this tuning burden or improve feasibility, including penalty and parameterization methods [16], adaptive variants such as Parameter-Adaptive CBF (PACBF) and Relaxation-Adaptive CBF (RACBF) [17], sampled-data adaptive CBFs [18], and learning-based designs of class \mathcal{K} functions [12,11]. Among sampled-data safety formulations, the zero-order CBF in [15] compares barrier values at consecutive sampling instants and predicts the next-step value through numerical approximation of the system flow. This enables high-relative-degree constraints but makes the safety condition implicit and sensitive to the accuracy of flow prediction.

We address the control-design complexity induced by high-relative-degree constraints and the resulting increase in tuning parameters for class \mathcal{K} functions. Our main contributions are:

- (1) We propose Truncated Taylor CBF (TTCBF), a new CBF variant that accommodates high-relative-degree safety constraints using only one class \mathcal{K} function, independent of the relative degree. We show that our TTCBF is a generalization of the standard discrete-time CBF, which can only consider safety constraints with relative degree one.
- (2) We further propose adaptive TTCBF (aTTCBF), an adaptive variant of our TTCBF that improves adaptability while requiring substantially fewer control-design parameters than existing adaptive variants of the standard HOCBF.

We validate our TTCBF and aTTCBF through numerical experiments with a spring-mass system with relative degree six and a corridor-navigation scenario with densely cluttered obstacles.

We adopt the following notation throughout the paper. Vectors are written in boldface. The indices $i \in \mathbb{N}$ and $j \in \mathbb{N}$ are reused with meanings defined locally. The index $k \in \mathbb{N}$ denotes discrete time steps, while $t := k\Delta t \in \mathbb{R}$ denotes a time instant with $\Delta t > 0$ being the sampling period of the controller.

The remainder of the paper is organized as follows. Section 2 introduces preliminaries for HOCBFs. Section 3 introduces our TTCBF and our aTTCBF based

on truncated Taylor expansions, which handle high-relative-degree safety constraints using only one class \mathcal{K} function. Section 4 reports numerical results, followed by discussions in Section 5 and conclusions in Section 6.

2 Preliminaries

We consider an input-affine control system of the form

$$\dot{\mathbf{x}} = f(\mathbf{x}) + g(\mathbf{x})\mathbf{u}, \quad (1)$$

where the system state is $\mathbf{x} := [x_1, \dots, x_n]^\top \in \mathcal{X} \subset \mathbb{R}^n$. The vector fields $f : \mathbb{R}^n \rightarrow \mathbb{R}^n$ and $g : \mathbb{R}^n \rightarrow \mathbb{R}^{n \times m}$ are assumed to be locally Lipschitz. The control input $\mathbf{u} := [u_1, \dots, u_m]^\top \in \mathcal{U} \subseteq \mathbb{R}^m$ is componentwise constrained as $\mathcal{U} := \{\mathbf{u} \in \mathbb{R}^m \mid \mathbf{u}_{\min} \leq \mathbf{u} \leq \mathbf{u}_{\max}\}$, where $\mathbf{u}_{\min}, \mathbf{u}_{\max} \in \mathbb{R}^m$ denote the minimum and maximum admissible control inputs, respectively.

In safety-critical control, the objective is to ensure that the system state \mathbf{x} remains within a prescribed (possibly time-varying) safe set $\mathcal{C}(t)$. Let $h : \mathcal{X} \times [t_0, \infty) \rightarrow \mathbb{R}$ be a continuously differentiable safety function, where $t_0 \in \mathbb{R}$ denotes an initial time. The safe set is defined as

$$\mathcal{C}(t) := \{\mathbf{x} \in \mathcal{X} \mid h(\mathbf{x}, t) \geq 0\}.$$

For system (1), define the gradient of h with respect to \mathbf{x} as $\nabla_{\mathbf{x}} h(\mathbf{x}, t) := \left[\frac{\partial h}{\partial x_1}, \dots, \frac{\partial h}{\partial x_n} \right]^\top$. The Lie derivatives of h along f and g are given by

$$L_f h(\mathbf{x}, t) := \nabla_{\mathbf{x}} h(\mathbf{x}, t)^\top f(\mathbf{x}), \quad (2)$$

$$L_g h(\mathbf{x}, t) := \nabla_{\mathbf{x}} h(\mathbf{x}, t)^\top g(\mathbf{x}). \quad (3)$$

For a time-varying safety function $h(\mathbf{x}, t)$, its time derivative along trajectories of (1) is

$$\dot{h}(\mathbf{x}, \mathbf{u}, t) = \frac{\partial h(\mathbf{x}, t)}{\partial t} + L_f h(\mathbf{x}, t) + L_g h(\mathbf{x}, t)\mathbf{u}.$$

Higher-order time derivatives $\frac{d^i}{dt^i} h(\mathbf{x}(t), t)$ are defined recursively by differentiating along trajectories of (1). Since standard CBF formulations require the control input to appear in the first derivative of the safety function, they are not applicable to safety constraints with higher relative degree. To formalize this notion, we adopt the following definition.

Definition 1 (Relative Degree [16]) *The relative degree $r \in \mathbb{N}$ of a sufficiently differentiable function $h : \mathcal{X} \times [t_0, \infty) \rightarrow \mathbb{R}$ with respect to system (1) is the smallest integer such that*

$$\frac{\partial}{\partial \mathbf{u}} \left(\frac{d^i}{dt^i} h(\mathbf{x}(t), t) \right) = \mathbf{0}_{1 \times m}, \quad \forall i \in \{0, \dots, r-1\}.$$

$$\frac{\partial}{\partial \mathbf{u}} \left(\frac{d^r}{dt^r} h(\mathbf{x}(t), t) \right) \neq \mathbf{0}_{1 \times m},$$

Definition 2 (Class \mathcal{K} function [16]) A function $\alpha : [0, b) \rightarrow [0, \infty)$, with $b > 0$, belongs to class \mathcal{K} if it is Lipschitz continuous, strictly increasing, and $\alpha(0) = 0$.

For a safety function h with relative degree r , the HOCBF proposed in [16] introduces a sequence of auxiliary functions

$$\begin{aligned} \Psi_0(\mathbf{x}, t) &:= h(\mathbf{x}, t), \\ \Psi_i(\mathbf{x}, t) &:= \dot{\Psi}_{i-1}(\mathbf{x}, t) + \alpha_i(\Psi_{i-1}(\mathbf{x}, t)), \quad \forall i \in \{1, \dots, r-1\}, \\ \Psi_r(\mathbf{x}, \mathbf{u}, t) &:= \dot{\Psi}_{r-1}(\mathbf{x}, \mathbf{u}, t) + \alpha_r(\Psi_{r-1}(\mathbf{x}, t)), \end{aligned} \quad (4)$$

where each $\alpha_i(\cdot)$ is a class \mathcal{K} function. Here, $\dot{\Psi}_i$ denotes the time derivative of Ψ_i along the system dynamics (1). By construction, the control input \mathbf{u} appears explicitly only in Ψ_r .

Based on (4), define the sets

$$\mathcal{C}_i(t) := \{\mathbf{x} \in \mathcal{X} \mid \Psi_{i-1}(\mathbf{x}, t) \geq 0\}, \quad \forall i \in \{1, \dots, r\}. \quad (5)$$

A set is said to be *forward invariant* for system (1) if every trajectory starting in the set remains in the set for all future time [16].

Definition 3 (HOCBFs [16]) A sufficiently differentiable function $h : \mathcal{X} \times [t_0, \infty) \rightarrow \mathbb{R}$ is an HOCBF of relative degree r for system (1) if there exist class \mathcal{K} functions $\alpha_i(\cdot)$, $i \in \{1, \dots, r\}$, such that

$$\sup_{\mathbf{u} \in \mathcal{U}} \Psi_r(\mathbf{x}, \mathbf{u}, t) \geq 0, \quad \forall (\mathbf{x}, t) \in \bigcap_{i=1}^r \mathcal{C}_i(t) \times [t_0, \infty). \quad (6)$$

Using (4), Ψ_r admits the explicit expression

$$\begin{aligned} \Psi_r(\mathbf{x}, \mathbf{u}, t) &= \mathcal{L}^r h(\mathbf{x}, t) + L_g \mathcal{L}^{r-1} h(\mathbf{x}, t) \mathbf{u} \\ &\quad + \sum_{i=1}^r \mathcal{L}^{i-1} \alpha_{r-i+1}(\Psi_{r-i}(\mathbf{x}, t)), \end{aligned} \quad (7)$$

where $\mathcal{L} := \partial_t + L_f$ denotes a differential operator, with ∂_t being the partial derivative with respect to time.

Since $\Psi_0 := h$, the set \mathcal{C}_1 coincides with the original safe set. As shown in [16], enforcing condition (6) ensures that $\Psi_i(\mathbf{x}, t) \geq 0$ for all $i \in \{0, \dots, r-1\}$, which renders the set $\bigcap_{i=1}^r \mathcal{C}_i(t)$ forward invariant for system (1).

3 Truncated Taylor-Based Formulation

We propose our TTCBF in Section 3.1 and aTTCBF in Section 3.2.

3.1 Truncated Taylor CBF (TTCBF)

The motivation for our TTCBF is that the standard HOCBF method proposed in [16] requires r class \mathcal{K} functions, where r is the relative degree of the safety constraint. The simplest choice is a linear class \mathcal{K} function $\alpha(h) = ah$ with $a > 0$ as a tuning parameter. Even with this choice, HOCBF still requires r class- \mathcal{K} parameters. This directly couples the number of tuning parameters with the relative degree of the safety constraint. Since the parameters of class \mathcal{K} functions directly determine the tightness of the safety constraint and the aggressiveness of the resulting control behavior (as demonstrated in Fig. 1), improper tuning can lead to degraded control performance or excessive conservatism. To simplify control synthesis and parameter tuning, we introduce our TTCBF, which decouples the number of tuning parameters from the relative degree.

Before we introduce our TTCBF, we define the notion of the relative degree in the discrete-time domain. Let $k \in \mathbb{N}$ denote the time step index and $t_k := k\Delta t$ the time instant, where $\Delta t > 0$ is the sampling period of the digital controller.

Definition 4 ([13]) Let $y(t_k) = h(\mathbf{x}(t_k), t_k)$ be a system output at time step k with $h : \mathcal{X} \times [t_0, \infty) \rightarrow \mathbb{R}$. The relative degree $r \in \mathbb{N}$ of y is the smallest integer such that

$$\begin{aligned} \frac{\partial y(t_{k+i})}{\partial \mathbf{u}(t_k)} &= \mathbf{0}_{1 \times m}, \quad \forall i \in \{0, \dots, r-1\}, \\ \frac{\partial y(t_{k+r})}{\partial \mathbf{u}(t_k)} &\neq \mathbf{0}_{1 \times m}. \end{aligned} \quad (8)$$

Informally, the relative degree r of a system output in discrete time is the number of time steps after which the control input $\mathbf{u}(t_k)$ first affects the output y . For systems with relative degree $r = 1$, the standard discrete-time CBF condition takes the form

$$h(\mathbf{x}(t_{k+1}), t_{k+1}) - h(\mathbf{x}(t_k), t_k) + \alpha(h(\mathbf{x}(t_k), t_k)) \geq 0, \quad (9)$$

where $\alpha(\cdot)$ is a class \mathcal{K} function satisfying $\alpha(s) \leq s$ for all $s \geq 0$ [1]. For outputs with relative degree $r > 1$, [18] extends this condition by cascading r class \mathcal{K} functions, in direct analogy to the continuous-time HOCBF construction in [16]. Below, we present a direct r -step generalization that involves only one class \mathcal{K} function. Before proceeding, we introduce the following proposition.

Proposition 5 Denote the discrete-time safe set

$$\mathcal{C}(t_k) := \{\mathbf{x}(t_k) \in \mathcal{X} \mid h(\mathbf{x}(t_k), t_k) \geq 0\} \quad (10)$$

for system (1). Let $k_0 \in \mathbb{N}$ be an initial time step, and assume the initial conditions

$$h(\mathbf{x}(t_{k_0+i}), t_{k_0+i}) \geq 0, \quad \forall i \in \{0, \dots, r-1\}. \quad (11)$$

Let $\alpha(\cdot)$ be a class \mathcal{K} function that satisfies $\alpha(s) \leq s$ for all $s \geq 0$. Assume that for every $k \geq k_0$ with $\mathbf{x}(t_k) \in \mathcal{C}(t_k)$, the controller applies an input $\mathbf{u}(t_k) \in \mathcal{U}$ such that

$$h(\mathbf{x}(t_{k+r}), t_{k+r}) - h(\mathbf{x}(t_k), t_k) + \alpha(h(\mathbf{x}(t_k), t_k)) \geq 0, \quad (12)$$

where $\mathbf{x}(t_{k+r})$ is the closed-loop state at time t_{k+r} under the applied inputs. Then $\mathcal{C}(t_k)$ is forward invariant for system (1), that is, $h(\mathbf{x}(t_k), t_k) \geq 0$ for all $k \geq k_0$.

PROOF. We prove $h(\mathbf{x}(t_k), t_k) \geq 0$ for all $k \geq k_0$ by induction. The base case for $k \in \{k_0, \dots, k_0+r-1\}$ holds by (11). For the inductive step, fix any $j \geq k_0+r-1$ and assume $h(\mathbf{x}(t_k), t_k) \geq 0$ for all $k \leq j$. Let $k' := j+1-r$, so that $k' \geq k_0$ and $k'+r = j+1$. Applying (12) at time step k' yields $h(\mathbf{x}(t_{j+1}), t_{j+1}) = h(\mathbf{x}(t_{k'+r}), t_{k'+r}) \geq h(\mathbf{x}(t_{k'}), t_{k'}) - \alpha(h(\mathbf{x}(t_{k'}), t_{k'}))$. By the induction hypothesis, $h(\mathbf{x}(t_{k'}), t_{k'}) \geq 0$. Using $\alpha(s) \leq s$ for $s \geq 0$ gives $h(\mathbf{x}(t_{k'}), t_{k'}) - \alpha(h(\mathbf{x}(t_{k'}), t_{k'})) \geq 0$, and therefore $h(\mathbf{x}(t_{j+1}), t_{j+1}) \geq 0$. This completes the induction. \square

Remark 6 For $r > 1$, Definition 4 implies that the control input chosen at time t_{k_0} does not affect $y(t_{k_0+i}) = h(\mathbf{x}(t_{k_0+i}), t_{k_0+i})$ for $i \in \{1, \dots, r-1\}$. Hence, condition (11) cannot be enforced by the control applied at time t_{k_0} . This role of initial nonnegativity is analogous to requiring nonnegative initial values of the auxiliary variables $\Psi_i(\mathbf{x}, t)$, $i \in \{0, \dots, r-1\}$, in the HOCBF construction (4).

$h(\mathbf{x}(t_{k+r}), \mathbf{u}(t_k), t_{k+r})$ in (12) is generally not an explicit function of the current control input $\mathbf{u}(t_k)$. A common approximation is to apply successive forward differences to obtain $h(\mathbf{x}(t_{k+i}), t_{k+i})$ from $i = 1$ until $i = r$ [18]. However, for non-linear systems, this often yields a non-affine dependence on $\mathbf{u}(t_k)$ that requires further approximation. Additionally, [18] relies on a cascade of class \mathcal{K} functions that require tuning. We circumvent these problems by expanding $h(\mathbf{x}(t_{k+r}), \mathbf{u}(t_k), t_{k+r})$ in a *truncated Taylor series* about $h(\mathbf{x}(t_k), t_k)$. Let the sampling period of the controller be $\Delta t > 0$ and define the Taylor step size

$$\Delta T := r\Delta t > 0. \quad (13)$$

Taylor's theorem gives

$$\begin{aligned} & h(\mathbf{x}(t_{k+r}), \mathbf{u}(t_k), t_{k+r}) \\ &= h(\mathbf{x}(t_k), t_k) + \sum_{i=1}^{r-1} \frac{(\Delta T)^i}{i!} h^{(i)}(\mathbf{x}(t_k), t_k) + \\ & \quad \frac{(\Delta T)^r}{r!} h^{(r)}(\mathbf{x}(t_k), \mathbf{u}(t_k), t_k) + R_T, \end{aligned} \quad (14)$$

where the remainder R_T admits the Lagrange form

$$R_T = \frac{(\Delta T)^{r+1}}{(r+1)!} h^{(r+1)}(\mathbf{x}(\tau), \mathbf{u}(\tau), \tau), \quad (15)$$

with $\tau \in (t_k, t_{k+r})$ being an intermediate time. We expand the Taylor series until the r -th derivative term because this is where \mathbf{u} explicitly appears. We choose ΔT as in (13) because the influence of $\mathbf{u}(t_k)$ to h is delayed by r time steps according to Definition 4. Now, we define our TTCBF as follows.

Definition 7 (Truncated Taylor CBF (TTCBF))
Let $h : \mathcal{X} \times [t_0, \infty) \rightarrow \mathbb{R}$ be an $(r+1)$ -times continuously differentiable function that defines a safe set $\mathcal{C}(t_k)$ as in (10) for system (1). Let $k_0 \in \mathbb{N}$ be an initial time step, and let the initial conditions (11) hold. Then, h is called a TTCBF of relative degree r for system (1) if there exists a class \mathcal{K} function $\alpha(\cdot)$ such that

$$\sup_{\mathbf{u}(t_k) \in \mathcal{U}} \left[\sum_{i=1}^{r-1} \frac{(\Delta T)^i}{i!} h^{(i)}(\mathbf{x}(t_k), t_k) + \frac{(\Delta T)^r}{r!} h^{(r)}(\mathbf{x}(t_k), \mathbf{u}(t_k), t_k) + R_T + \alpha(h(\mathbf{x}(t_k), t_k)) \right] \geq 0 \quad (16)$$

holds for every $k \geq k_0$ with $\mathbf{x}(t_k) \in \mathcal{C}(t_k)$.

In (16), the remainder R_T is unknown since the intermediate time τ in (15) is unknown. We tackle this problem with the following theorem.

Theorem 8 Let h be a TTCBF with relative degree r for system (1) with the associated safe set $\mathcal{C}(t_k)$ as in Definition 7. Let ΔT be a Taylor step size as in (13). Any Lipschitz continuous controller satisfying

$$\begin{aligned} & \sum_{i=1}^{r-1} \frac{(\Delta T)^i}{i!} h^{(i)}(\mathbf{x}(t_k), t_k) + \frac{(\Delta T)^r}{r!} h^{(r)}(\mathbf{x}(t_k), \mathbf{u}(t_k), t_k) \\ & \quad + \alpha(h(\mathbf{x}(t_k), t_k)) + \inf_{\mathbf{u}(t_k) \in \mathcal{U}} R_T \geq 0 \end{aligned} \quad (17)$$

renders $\mathcal{C}(t_k)$ forward invariant for system (1).

PROOF. Substituting (14) into (12) yields

$$\begin{aligned} & \sum_{i=1}^{r-1} \frac{(\Delta T)^i}{i!} h^{(i)}(\mathbf{x}(t_k), t_k) + \frac{(\Delta T)^r}{r!} h^{(r)}(\mathbf{x}(t_k), \mathbf{u}(t_k), t_k) \\ & \quad + \alpha(h(\mathbf{x}(t_k), t_k)) + R_T \geq 0. \end{aligned} \quad (18)$$

Since (17) considers the worst-case (most negative) R_T over all admissible control inputs \mathcal{U} , thus (17) is a sufficient condition for (18). Given Proposition 5, $\mathcal{C}(t_k)$ is forward invariant for system (1). \square

To compute the term $\inf_{\mathbf{u}(t_k) \in \mathcal{U}} R_T$ in (17), we denote $h_{k,\min}^{(i)} := \inf_{\mathbf{u}(t_k) \in \mathcal{U}} h^{(i)}(\mathbf{x}(t_k), \mathbf{u}(t_k), t_k)$ for $i \in \{r, r+1\}$. Given (15), applying the backward difference $h_{k,\min}^{(r+1)} = (h_{k,\min}^{(r)} - h_{k-1}^{(r)})/\Delta t$ yields

$$\begin{aligned} \inf_{\mathbf{u}(t_k) \in \mathcal{U}} R_T &= \frac{(\Delta T)^{r+1}}{(r+1)!} h_{k,\min}^{(r+1)} \\ &= \frac{(\Delta T)^{r+1}}{(r+1)!\Delta t} \left(h_{k,\min}^{(r)} - h_{k-1}^{(r)} \right), \end{aligned} \quad (19)$$

where $h_{k-1}^{(r)}$ denotes the r -th time derivative of h at the previous time step $k-1$, which is known at the current time k . Next, we discuss how to determine $h_{k,\min}^{(r)}$. For input-affine systems like (1), the r -th time derivative of h depends on the control input $\mathbf{u}(t_k)$ in an affine manner. Consequently, computing $h_{k,\min}^{(r)}$ reduces to minimizing an affine function of $\mathbf{u}(t_k)$ over the admissible set \mathcal{U} . If \mathcal{U} is a polytope (defined by linear inequalities), this minimization is a linear program and can be solved efficiently online. If \mathcal{U} is a norm ball (e.g., $\|\mathbf{u}\|_2 \leq u_{\max}$), minimizing an affine function over \mathcal{U} often admits a closed-form solution [5, Appendix A.1.6]. However, if the dependence on \mathbf{u} is non-affine or if \mathcal{U} is defined by nonlinear nonconvex constraints, the minimization becomes a generally nonconvex nonlinear program, which limits the applicability of our approach in such cases.

Remark 9 For safety constraints with relative degree $r = 1$, (11) becomes $h(\mathbf{x}(t_{k_0}), t_{k_0}) \geq 0$ and (12) reduces to the standard discrete-time CBF condition (9) proposed in [1]. Therefore, our TTCBF generalizes the standard discrete-time CBF to high-order safety constraints.

3.2 Adaptive TTCBF (aTTCBF)

Safety-critical controllers often operate in changing environments. Adaptive CBFs address this setting by adjusting the class \mathcal{K} function online, which in turn modifies the closed-loop behavior. For HOCBF, however, the number of class \mathcal{K} functions scales with the relative degree of the safety constraint, so the control-design complexity of existing adaptive variants of HOCBF also scales with the relative degree. In contrast, our TTCBF uses only one class \mathcal{K} function, which simplifies the construction of adaptive variants. In this section, we introduce an adaptive variant of our TTCBF, termed aTTCBF.

Definition 10 (adaptive TTCBF (aTTCBF)) Let $h : \mathcal{X} \times [t_0, \infty) \rightarrow \mathbb{R}$ be an $(r+1)$ -times continuously

differentiable function that defines a safe set $\mathcal{C}(t_k)$ as in (10) for system (1). Let $k_0 \in \mathbb{N}$ be an initial time step, and let the initial condition (11) hold. Then, h is called an aTTCBF of relative degree r for system (1) if there exists a class \mathcal{K} function $\hat{\alpha}(\cdot)$ such that

$$\begin{aligned} \sup_{\mathbf{u}(t_k) \in \mathcal{U}} \left[\sum_{i=1}^{r-1} \frac{(\Delta T)^i}{i!} h^{(i)}(\mathbf{x}(t_k), t_k) + \right. \\ \left. \frac{(\Delta T)^r}{r!} h^{(r)}(\mathbf{x}(t_k), \mathbf{u}(t_k), t_k) + \right. \\ \left. R_T + \underbrace{\eta(t_k) \hat{\alpha}(h(\mathbf{x}(t_k), t_k))}_{\alpha(h, t_k)} \right] \geq 0 \end{aligned} \quad (20)$$

holds for every $k \geq k_0$ with $(\mathbf{x}(t_k), t_k) \in \mathcal{C}(t_k) \times [t_{k_0}, \infty)$. Here, $\hat{\alpha}(\cdot)$ is a coefficient-free class \mathcal{K} function satisfying $\hat{\alpha}(h) \leq h$, i.e., whose scaling gain is normalized to one, and $\eta(t_k) \in [0, 1]$ is an adaptive gain.

Essentially, we separate the class \mathcal{K} function $\alpha(h, t_k)$ into two multiplicative parts: a gain $\eta(t_k)$ and a coefficient-free class \mathcal{K} function $\hat{\alpha}(\cdot)$. Conventionally, this gain is a parameter that must be manually tuned. In our aTTCBF, we use an adaptive gain $\eta(t_k)$ that is optimized online. We have a theorem for our aTTCBF similar to Theorem 8 for our TTCBF as follows.

Theorem 11 Let h be an aTTCBF with relative degree r for system (1) with the associated safe set $\mathcal{C}(t_k)$ as in Definition 10. Let ΔT be a Taylor step size as in (13). Any Lipschitz continuous controller satisfying

$$\begin{aligned} \sum_{i=1}^{r-1} \frac{(\Delta T)^i}{i!} h^{(i)}(\mathbf{x}(t_k), t_k) + \frac{(\Delta T)^r}{r!} h^{(r)}(\mathbf{x}(t_k), \mathbf{u}(t_k), t_k) \\ + \eta(t_k) \hat{\alpha}(h(\mathbf{x}(t_k), t_k)) + \inf_{\mathbf{u}(t_k) \in \mathcal{U}} R_T \geq 0 \end{aligned} \quad (21)$$

renders $\mathcal{C}(t_k)$ forward invariant for system (1).

PROOF. Since $\hat{\alpha}(\cdot)$ satisfies $\hat{\alpha}(h) \leq h$ and $\eta(t_k) \in [0, 1]$, the inequality $\alpha(h, t_k) \leq h$ holds, which is required by the standard discrete-time CBFs (9). The remaining proof follows directly from the proof of Theorem 8. \square

3.3 Optimal Control Problem Formulation

We assume that a nominal controller exists whose safety we seek to certify, while minimizing the deviation from its behavior. For our TTCBF and aTTCBF, we formulate a CLF-CBF-QP [4] that is solved at each time step k . For clarity, we present the case with one safety constraint. One can extend the formulation to multiple safety constraints by adding the corresponding safety

constraints to the QP and augmenting the cost with additional penalty terms.

$$\arg \min_{\substack{\mathbf{u}(t_k) \in \mathcal{U}, \\ \zeta(t_k) \geq 0, \\ \eta(t_k) \in [0,1]}} \|\mathbf{u}(t_k) - \mathbf{u}_{\text{nom}}(t_k)\|_{W_u}^2 + w_\zeta \zeta(t_k)^2 + \underbrace{w_\eta \eta(t_k)^2}_{\text{aTTCBF only}} \quad (22a)$$

s.t.

Safety: (17) for TTCBF, or (21) for aTTCBF (22b)

Stability: $\dot{V}(\mathbf{x}(t_k)) + \alpha_L(V(\mathbf{x}(t_k))) \leq \zeta(t_k)$ (22c)

In (22a), $W_u \in \mathbb{R}^{m \times m} \succ 0$ penalizes the deviation of the optimized control $\mathbf{u}(t_k)$ from the nominal input $\mathbf{u}_{\text{nom}}(t_k)$. If a nominal controller is unavailable, one can omit $\mathbf{u}_{\text{nom}}(t_k)$ so that this term penalizes control effort. The slack variable $\zeta(t_k) \geq 0$ relaxes the CLF constraint (22c) and is penalized by $w_\zeta > 0$. For aTTCBF, the additional term with weight $w_\eta > 0$ penalizes the adaptive gain $\eta(t_k) \in [0, 1]$ in (21). Alternatively, one can introduce a nominal adaptive gain and penalize deviations from it. Note that the $\eta(t_k)$ only exists in (22a) for aTTCBF. The stability constraint (22c) enforces convergence of $\mathbf{x}(t_k)$ toward a desired state $\mathbf{x}_{\text{des}}(t_k)$ via a CLF, where $\alpha_L(\cdot)$ is a class \mathcal{K} function. A common choice is $V(\mathbf{x}(t_k)) = \|\mathbf{x}(t_k) - \mathbf{x}_{\text{des}}(t_k)\|_2^2$. Without loss of generality, we assume that the CLF has relative degree one. If this assumption does not hold, one can use a high-order CLF constructed analogously to high-order CBFs, which we ignore for brevity.

Remark 12 (Adaptability of aTTCBF) *The adaptability of our aTTCBF arises from the decision variable $\eta(t_k)$ in (22). It acts as an adaptive gain of the class \mathcal{K} function in (21). The quadratic penalty $w_\eta \eta(t_k)^2$ encourages small values of $\eta(t_k)$ while allowing $\eta(t_k)$ to increase when necessary to maintain feasibility. When (21) becomes infeasible under the control bounds \mathcal{U} , increasing $\eta(t_k)$ relaxes the constraint. Conversely, when the safety constraint is inactive, for example, when the system state is far from the safety boundary, the optimizer reduces $\eta(t_k)$ to limit the allowed rate at which the system state approaches the safety boundary, that is, to limit the decay rate of the barrier value. This mechanism provides a continuous adjustment of conservatism that can improve feasibility under tight control bounds.*

4 Numerical Experiments

We conduct numerical experiments to support our theoretical results and to validate the proposed TTCBF and aTTCBF. In Section 4.1, we demonstrate that our TTCBF can handle safety constraints with high relative degree using a serial spring-mass system whose safety constraint has relative degree six. In Section 4.2, we illustrate the applicability of our TTCBF and aTTCBF

to different types of class \mathcal{K} functions in a corridor-navigation scenario. In the same scenario, we compare our aTTCBF with PACBF and RACBF, two adaptive variants proposed in [17] for HOCBF [16], and show improved adaptability of our aTTCBF. All simulations are implemented in Python and executed on an Apple M2 Pro with 16 GB RAM. We formulate and solve the QPs using CVXPY [7]. The code to reproduce our results, together with video demonstrations, is publicly available¹.

4.1 Spring-Mass System: Relative Degree Six

We evaluate our TTCBF on the serial spring-mass benchmark introduced in [14], which features a safety constraint with relative degree six. Fig. 2a illustrates the setup. Three identical point masses m_1, m_2 , and m_3 of 1.0 kg move along a horizontal line and are connected by identical linear springs of stiffness $k = 5.0 \text{ N/m}$. An external force u bounded by $|u| \leq 5 \text{ N}$ acts on the first mass m_1 . Let x_i denote the horizontal position of each mass i . The system dynamics are

$$\begin{aligned} m_1 \ddot{x}_1 &= u + k(x_2 - x_1), \\ m_2 \ddot{x}_2 &= k(x_1 - x_2) + k(x_3 - x_2), \\ m_3 \ddot{x}_3 &= k(x_2 - x_3). \end{aligned}$$

With the state vector $\mathbf{x} = [x_1, x_2, x_3, \dot{x}_1, \dot{x}_2, \dot{x}_3]^\top \in \mathbb{R}^6$, the system is linear time-invariant, $\dot{\mathbf{x}} = A\mathbf{x} + B\mathbf{u}$, where

$$A = \begin{bmatrix} \mathbf{0}_{3 \times 3} & I_3 \\ A' & \mathbf{0}_{3 \times 3} \end{bmatrix}, \quad A' = \begin{bmatrix} -\frac{k}{m_1} & \frac{k}{m_1} & 0 \\ \frac{k}{m_2} & -\frac{2k}{m_2} & \frac{k}{m_2} \\ 0 & \frac{k}{m_3} & -\frac{k}{m_3} \end{bmatrix}, \quad B = \begin{bmatrix} \mathbf{0}_{3 \times 1} \\ \frac{1}{m_1} \\ \mathbf{0}_{2 \times 1} \end{bmatrix},$$

with I_3 denoting an identity matrix of size 3.

The control objective is to steer the third mass to a desired position $x_{3,\text{des}} = 3.0 \text{ m}$ while enforcing the safety constraint $x_3 \leq x_{3,\text{safe}} = 3.5 \text{ m}$. We define the safe set as $\mathcal{C} = \{\mathbf{x} : h(\mathbf{x}) := x_{3,\text{safe}} - x_3 \geq 0\}$. Therefore, the input u must propagate through two springs and three double integrators. One can easily show that h has relative degree six with respect to the system dynamics. We use sampling period $\Delta t = 0.01 \text{ s}$ and set the initial state $\mathbf{x}_0 = [0, 1, 2, 2, 1, 0]^\top$.

To assess the effectiveness of our TTCBF, we implement two controllers: 1) a *nominal controller* with I/O-linearization that aims at following $x_{3,\text{des}}$ and ignores safety, and 2) a CBF-QP-based controller employing our TTCBF that aims to certify the safety of the nominal controller, referred to as *our controller* thereafter. We design the nominal controller using exact input-output linearization followed by pole placement. Let the system output be $y := C_y \mathbf{x} = x_3$, where $C_y = [0, 0, 1, 0, 0, 0]$.

¹ <https://github.com/bassamlab/ttcbf>

Since y has relative degree six, the input-output dynamics can be expressed as $y^{(6)} = C_y A^6 \mathbf{x} + C_y A^5 B u$. Defining the tracking error $e^{(i)} := y^{(i)} - y_{\text{ref}}^{(i)}$ with output reference $y_{\text{ref}} = x_{3,\text{des}}$, we specify the desired error dynamics as $e^{(6)} + a_5 e^{(5)} + a_4 e^{(4)} + a_3 e^{(3)} + a_2 e^{(2)} + a_1 e^{(1)} + a_0 e = 0$, where the coefficients a_i correspond to the expanded form of $(s + \lambda)^6$ for a chosen pole location $\lambda > 0$ (which we tune as $\lambda = 2.0$). The resulting control law is

$$u = \frac{e^{(6)} - C_y A^6 \mathbf{x}}{C_y A^5 B}, \text{ where } e^{(6)} = - \sum_{i=0}^5 a_i e^{(i)}.$$

In our controller, we define $\arg \min_{u \in \mathcal{U}} (u - u_{\text{nom}})^2$ as the cost function, which optimizes the control u such that it minimally deviates from the nominal control input u_{nom} while respecting the safety constraint (18) imposed by our TTCBF. For (18), we apply a linear class \mathcal{K} function $\alpha(h) = \lambda h$ with $\lambda = 0.95$ (after proper tuning).

Results: Fig. 2b depicts the positions of each mass m_i , and the position of m_3 is shown in solid lines. Both controllers are able to track the desired position $x_{3,\text{des}}$ for mass m_3 . However, the nominal controller (gray) overshoots and reaches $x_3 = 4.0$ m at $t = 2.6$ s, thereby violating the safety bound by 0.4 m. Our controller (cyan) successfully prevents this violation. Fig. 2c shows the applied control u . Up to $t = 0.57$ s, both controllers apply the same input because the nominal control is safe, and thus our TTCBF is inactive. After this time instance, it becomes active and reduces u so that mass m_1 pushes m_2 less aggressively, and m_3 approaches the safety boundary gently, reaching $x_{3,\text{safe}}$ at $t = 1.9$ s without overshoot.

4.2 Corridor Navigation

In Section 4.2.1, we evaluate how TTCBF accommodates different class \mathcal{K} functions in a corridor-navigation scenario and demonstrate the adaptability of aTTCBF by comparing it with TTCBF. In the same scenario, we further benchmark our aTTCBF against two adaptive variants proposed in [17], namely PACBF and RACBF.

The task is to control a robot to follow the circular corridor centerline (radius 40 m) counterclockwise at the desired speed $v_{\text{des}} = 10$ m/s, while avoiding collisions with the inner and outer corridor boundaries and with a set of $n_{\text{obs}} = 16$ circular obstacles placed along both boundaries, as shown in Fig. 4a. The robot is modeled with the nonlinear unicycle model

$$\dot{\mathbf{x}} = \begin{bmatrix} \dot{x} \\ \dot{y} \\ \dot{\theta} \\ \dot{v} \end{bmatrix} = \begin{bmatrix} v \cos \theta \\ v \sin \theta \\ u_1 \\ u_2 \end{bmatrix}, \quad \mathbf{x} = \begin{bmatrix} x \\ y \\ \theta \\ v \end{bmatrix}, \quad \mathbf{u} = \begin{bmatrix} u_1 \\ u_2 \end{bmatrix}, \quad (23)$$

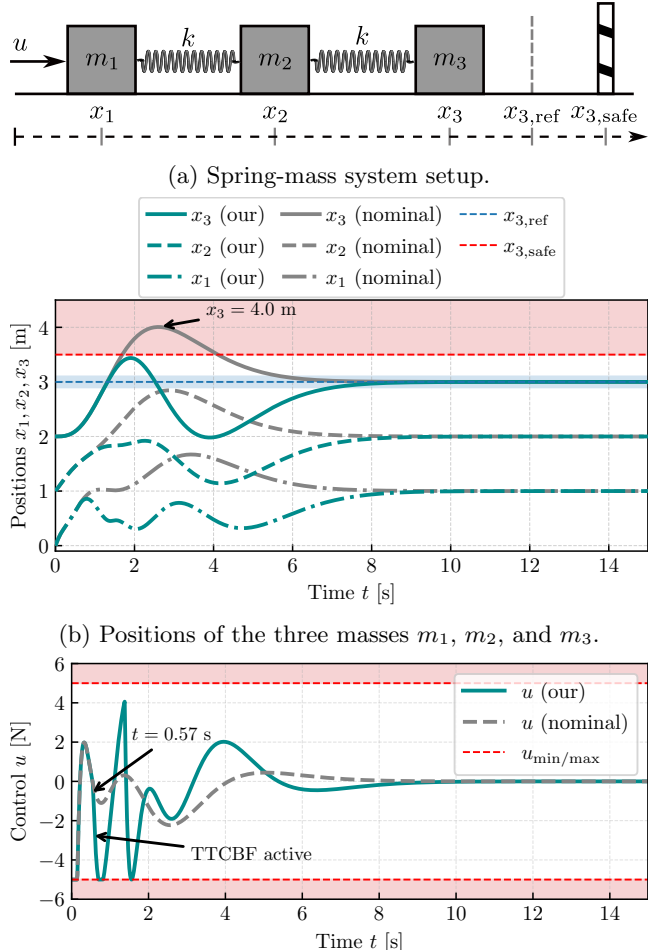


Fig. 2. Spring-mass system controlled by the nominal and our controller. Forbidden areas are shown in red.

where (x, y) is the position, θ the heading, v the longitudinal speed, u_1 the steering rate, and u_2 the longitudinal acceleration. We use the sampling period $\Delta t = 0.05$ s.

We define the safe sets using signed distances between the robot and the corridor boundaries and between the robot and the obstacles. The resulting CBFs have relative degree two with respect to the system dynamics. Specifically, for the inner boundary, we use

$$h = (x - x_c)^2 + (y - y_c)^2 - (r_{\text{inn}} + r_{\text{rob}})^2,$$

and for the outer boundary, we use

$$h = (r_{\text{out}} - r_{\text{rob}})^2 - (x - x_c)^2 - (y - y_c)^2,$$

where $(x_c, y_c) = (0 \text{ m}, 0 \text{ m})$ is the corridor center and $r_{\text{inn}} = 35 \text{ m}$, $r_{\text{out}} = 45 \text{ m}$, and $r_{\text{rob}} = 2 \text{ m}$ are the radii of the inner boundary, outer boundary, and robot, respectively. For each obstacle $i \in \{0, \dots, n_{\text{obs}} - 1\}$, we define

$$h = (x - x_i)^2 + (y - y_i)^2 - (r_{i,\text{obs}} + r_{\text{rob}})^2,$$

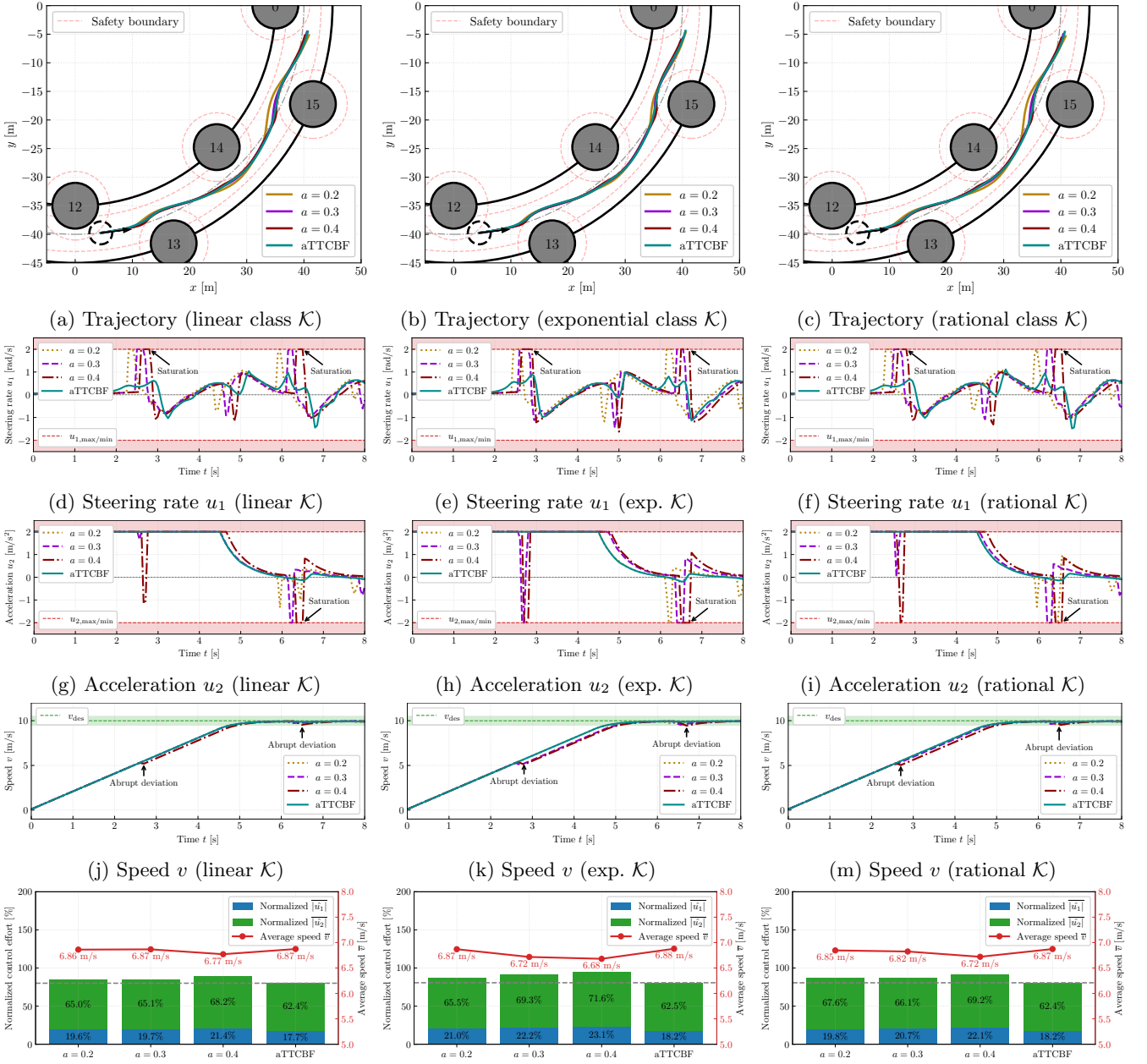


Fig. 3. Corridor navigation with our TTCBF and aTTCBF with a linear (1st column), an exponential (2nd column), and a rational (3rd column) class \mathcal{K} functions. The 1st row: robot trajectories; 2nd row: steering rate u_1 . 3rd row: acceleration u_2 . 4th row: speed v . 5th row: normalized control effort \bar{u} and average speed \bar{v} .

where (x_i, y_i) is the obstacle center and $r_{i,\text{obs}} = 4\text{ m}$ is the obstacle radius. The red dashed circles in Fig. 4a indicate the zero-level sets of these CBFs, obtained by inflating the corridor boundaries and obstacles by the robot radius. Any intersection between the robot trajectory and these circles indicates a violation of the safety constraints.

We use two CLFs to track the corridor centerline (gray

dash-dotted lines in Fig. 4a). At each time step, we sample a target point on the centerline ahead of the robot by 5.0° and define a desired heading θ_{des} pointing from the robot toward this point. We set $V_\theta = e_\theta^2$ with $e_\theta = \theta - \theta_{\text{des}}$ for heading tracking, and $V_v = e_v^2$ with $e_v = v - v_{\text{des}}$ for speed tracking. The corresponding CLF constraints are $\dot{V}_\theta + \lambda_{L,v} V_v \leq \zeta_v$ and $\dot{V}_\theta + \lambda_{L,\theta} V_\theta \leq \zeta_\theta$, where $\dot{V}_\theta = 2(\theta - \theta_{\text{des}})u_1$, $\dot{V}_v = 2(v - v_{\text{des}})u_2$, $\lambda_{L,v} = \lambda_{L,\theta} = 4.0$, and $\zeta_\theta \geq 0$, $\zeta_v \geq 0$ are CLF relaxation variables. The

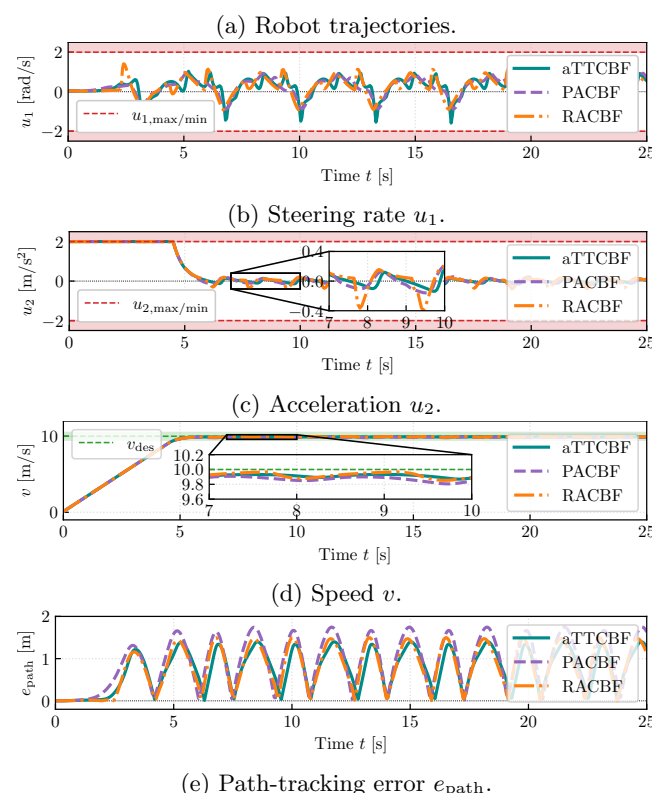
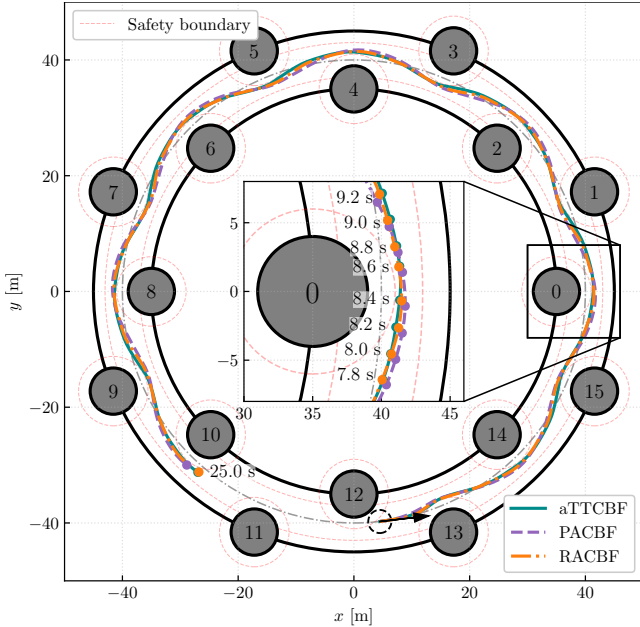


Fig. 4. Comparing aTTCBF (our), PACBF, and RACBF: (a) trajectories, (b-c) control inputs, (d-e) control performance.

cost function follows (22a). We use a proportional nominal controller $\mathbf{u}_{\text{nom}} = [K_\theta e_\theta, K_v e_v]^\top$ with $K_\theta = 1.0$ and $K_v = 1.0$. The weights for penalizing the deviation from \mathbf{u}_{nom} , the relaxation variables, and the aTTCBF adaptive gains are 1, 100, and 500, respectively.

(Continued from Fig. 4)

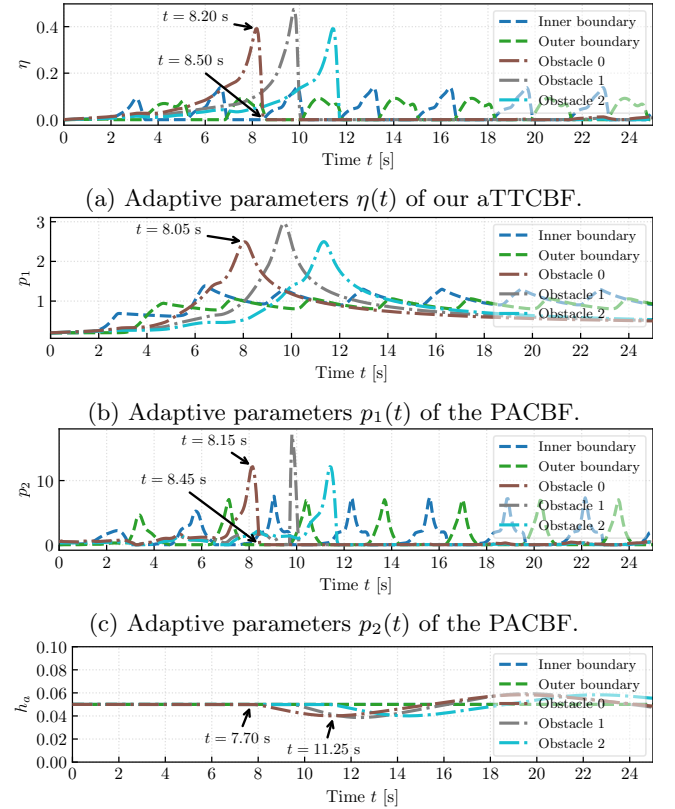


Fig. 5. Comparing aTTCBF (our), PACBF, and RACBF: (a-d) adaptive parameters of five selected safety constraints (two corridor boundaries and three obstacles).

4.2.1 Comparing aTTCBF with TTCBF

We compare aTTCBF with the non-adaptive TTCBF under different class \mathcal{K} functions. For TTCBF, the safety constraint is (17), while for aTTCBF it is (21). We consider three class \mathcal{K} functions: 1) linear: $\alpha(h) = ah$ for TTCBF and $\alpha(h, t) = \eta(t)h$ for aTTCBF; 2) exponential: $\alpha(h) = ah^{1.1}$ for TTCBF and $\alpha(h, t) = \eta(t)h^{1.1}$ for aTTCBF; and 3) rational: $\alpha(h) = a\frac{h^2}{1+h}$ for TTCBF and $\alpha(h, t) = \eta(t)\frac{h^2}{1+h}$ for aTTCBF. For each type, we test $a \in \{0.2, 0.3, 0.4\}$, and aTTCBF adapts $\eta(t) \in [0, 1]$ online. Each simulation runs for 8.0 s.

Safety: As shown in Figs. 3a–3c, both TTCBF and aTTCBF avoid collisions for all tested parameters, as the trajectories do not intersect the safety boundaries shown by red dashed circles.

Speed-tracking performance: Across all tested settings, aTTCBF yields improved speed tracking relative to TTCBF. In Figs. 3j–3m, aTTCBF converges smoothly toward v_{des} , whereas TTCBF occasionally exhibits abrupt deviations after reaching the desired

speed. We also compare the average speed, and an average speed closer to the desired speed $v_{\text{des}} = 10.0 \text{ m/s}$ indicates better speed tracking. The average-speed curves (red) in Figs. 3n–3p confirm that aTTCBF achieves higher average speed in all cases.

Control effort: Figs. 3d–3i show that the control inputs under aTTCBF are consistently smoother than under TTCBF. For the linear class \mathcal{K} function, Fig. 3d shows that the steering rate u_1 under TTCBF saturates at the upper bound twice, whereas aTTCBF avoids these saturations. Similarly, Fig. 3g shows that the acceleration u_2 under TTCBF reaches its lower bound once, while aTTCBF does not. Similar behavior is observed for the exponential class \mathcal{K} function in Figs. 3e–3h and for the rational class \mathcal{K} function in Figs. 3f–3i. We quantify control effort using the average magnitudes of u_1 and u_2 , normalized by the limits $u_{1,\text{max}} = 2.0 \text{ rad/s}$ and $u_{2,\text{max}} = 2.0 \text{ m/s}^2$, denoted by $|\hat{u}_1|$ and $|\hat{u}_2|$. The gray dashed horizontal lines in Figs. 3n–3p show that aTTCBF requires less total control effort across all tested parameters. For example, with the linear class \mathcal{K} function, aTTCBF yields $|\hat{u}_1| = 17.7\%$ and $|\hat{u}_2| = 62.4\%$, which are lower than the corresponding values for TTCBF across all tested a . Similar trends hold for the exponential and rational cases.

In summary, compared with TTCBF, aTTCBF yields improved speed tracking and reduced control effort across all tested class \mathcal{K} functions. This improvement comes with a modest computational overhead: the average QP solving time increases from 0.75 ms per step for TTCBF to 0.87 ms per step for aTTCBF, corresponding to a 16.0% increase. In Section 4.2.2, we show that this overhead is smaller than that of other adaptive variants, namely PACBF and RACBF.

4.2.2 Comparing aTTCBF with PACBF and RACBF

We compare our aTTCBF with PACBF and RACBF from [17]. All methods use well-tuned parameters, and each simulation runs for 25.0 s.

Safety and control effort: Fig. 4a shows that all three methods avoid collisions. The control inputs are shown in Figs. 4b and 4c. Overall, the three methods exhibit similar trends. Our aTTCBF uses slightly larger negative values of u_1 (cyan curve in Fig. 4b), while RACBF requires noticeably larger negative values of u_2 (orange curve in Fig. 4c). In terms of control effort, aTTCBF yields $|\hat{u}_1| = 0.45 \text{ rad/s}$ and $|\hat{u}_2| = 0.45 \text{ m/s}^2$, PACBF yields $|\hat{u}_1| = 0.43 \text{ rad/s}$ and $|\hat{u}_2| = 0.47 \text{ m/s}^2$, and RACBF yields $|\hat{u}_1| = 0.44 \text{ rad/s}$ and $|\hat{u}_2| = 0.49 \text{ m/s}^2$. Normalizing by $u_{1,\text{max}} = 2.0 \text{ rad/s}$ and $u_{2,\text{max}} = 2.0 \text{ m/s}^2$ and summing the two components, aTTCBF and PACBF each use 45.0% of the control capacity, while RACBF uses 46.5%.

Speed- and path-tracking performance: Figs. 4d and 4e show the speed-tracking performance and the centerline path-tracking error, respectively. The speed profiles are similar for all three methods (Fig. 4d). The average speeds are 8.94 m/s for aTTCBF (89.4% of v_{des}), 8.90 m/s for PACBF (89.0%), and 8.94 m/s for RACBF (89.4%). Because the obstacles densely constrain the feasible state space, the robot must deviate from the centerline when avoiding obstacles, so perfect centerline tracking is not achievable. We quantify path tracking using the absolute mean centerline deviation e_{path} . As shown in Fig. 4e, our aTTCBF reduces the mean path-tracking error from 0.95 m (PACBF) and 0.79 m (RACBF) to 0.76 m, which corresponds to reductions of 20.0% and 3.8%, respectively.

Adaptability: Our aTTCBF uses one adaptive parameter $\eta(t)$. The PACBF uses two adaptive parameters, denoted by $p_1(t)$ and $p_2(t)$, while the RACBF uses one adaptive parameter $h_a(t)$ [17]. Figs. 5a–5d show these parameters for the safety constraints associated with the inner and outer corridor boundaries and three representative obstacles. In Fig. 5a, $\eta(t)$ for obstacle 0 (brown dash-dotted line) increases as the robot approaches the obstacle, peaks at $t = 8.20 \text{ s}$, and decreases to zero at $t = 8.50 \text{ s}$. This decrease occurs because, once the robot passes the closest point (see the zoomed view in Fig. 4a) at $t = 8.50 \text{ s}$, the barrier value stops decreasing and a smaller $\eta(t)$ suffices to maintain the feasibility of the QP (22). As the robot moves away, the barrier value increases and the optimizer drives $\eta(t)$ to zero due to the quadratic penalty in (22a). Similar behavior is observed for obstacles 1 and 2.

Figs. 5b and 5c show that $p_1(t)$ and $p_2(t)$ exhibit similar trends but can peak at different times. For obstacle 0, $p_1(t)$ peaks at 8.05 s, while $p_2(t)$ peaks at 8.15 s. This behavior illustrates a practical drawback of using multiple adaptive parameters: although the parameters adapt online, the corresponding penalty weights in the cost function must still be tuned, which complicates the control design. We report the best performance obtained after extensive tuning.

Fig. 5d shows the adaptive parameter $h_a(t)$ for RACBF. It is initialized at 0.05 and regulated toward the same desired value. As observed, $h_a(t)$ decreases at 7.70 s to relax the constraint associated with obstacle 0 and increases again at 11.25 s to return toward the desired value. The adaptation in RACBF starts earlier than in aTTCBF and PACBF, and its response is slower.

Computational time and control-design parameters: The average QP solving time for our aTTCBF is 0.71 ms per step, which is a 54.5% reduction compared to PACBF (1.56 ms) and a 9.0% reduction compared to RACBF (0.78 ms). In addition, in this scenario, our aTTCBF requires 18 control-design parameters that are related to class \mathcal{K} functions, which is a 75.0% reduction

Table 1
Overview of the comparison of our aTTCBF, the PACBF [17], and the RACBF [17].

Methods	Control effort	Speed tracking	Path tracking	QP-sol. time	#Design param.
Our aTTCBF	45.0%	89.4%	0.76m	0.71ms	18
PACBF [17]	45.0%	89.0 %	0.95 m	1.56 ms	72
RACBF [17]	46.5 %	89.4%	0.79 m	0.78 ms	126

relative to PACBF (72 parameters) and a 85.7% reduction relative to RACBF (126 parameters). We refer to Appendix A for detailed computation.

Table 1 summarizes the performance of our aTTCBF, the PACBF, and the RACBF. Overall, our aTTCBF achieves the best speed- and path-tracking performance while requiring the lowest computation time and the fewest control-design parameters. Control effort is comparable between aTTCBF and PACBF, and both are slightly lower than RACBF.

5 Discussions

Compared with the HOCBF in [16], our TTCBF in Section 3.1 offers a key advantage: it accommodates safety constraints with high relative degree using only one class \mathcal{K} function. This yields two benefits. First, the number of class \mathcal{K} functions that require tuning is one, independent of the relative degree of the safety constraint. Second, adaptive variants based on our TTCBF, such as our aTTCBF, are substantially less complex than existing adaptive variants, including PACBF and RACBF [17].

A limitation of our TTCBF is that the Taylor size $\Delta T = r\Delta t$ (see (13)) is coupled with both the controller sampling period Δt and the relative degree r of the safety constraint. As shown in (17), the r -th Taylor term $h^{(r)}$, which is the first term that depends on the control input, is scaled by $(\Delta T)^r/r!$. When r is large and $\Delta T < 1.0$ s, this coefficient can become very small, which may lead to numerical ill-conditioning in the resulting QP. We consider two remedies that increase ΔT . The first is to increase the sampling period Δt . If a larger Δt is not feasible, a second approach is to redefine the Taylor size as $\Delta T = r'\Delta t$ with a chosen integer $r' > r$. The second approach introduces a “look-ahead” effect to time step $k+r'$ by zero-order holding the control input over the additional steps, that is, by setting $\mathbf{u}(t_{k+1}), \dots, \mathbf{u}(t_{k+r'-r})$ equal to $\mathbf{u}(t_k)$. This look-ahead mitigates the myopic nature of standard CBFs [16]. With an enlarged Taylor size, our TTCBF resembles a receding-horizon formulation in which the control horizon is one and the input beyond the horizon is held constant, resembling the idea in Model Predictive Control (MPC) with a control horizon of one. We have not yet established a theoretical analysis for our TTCBF under this enlarged Taylor size and will address it in future work.

6 Conclusions

In this work, we proposed Truncated Taylor CBF (TTCBF), which generalizes the standard discrete-time CBF to consider safety constraints with high relative degree. Different from the existing HOCBF that employs a chain of class \mathcal{K} functions, our TTCBF uses only one. Further, we propose an adaptive variant for our TTCBF—adaptive TTCBF (aTTCBF). Since the number of tuned class \mathcal{K} functions is independent of the relative degree, our TTCBF and aTTCBF reduce control-design complexity compared with HOCBF and its adaptive variants, PACBF and RACBF. We successfully demonstrated that our TTCBF handles a relative-degree-six safety constraint on a spring-mass system. In a corridor-navigation scenario, we demonstrated that our TTCBF and aTTCBF are able to accommodate different class \mathcal{K} functions (linear, exponential, and rational). Moreover, our aTTCBF outperforms PACBF and RACBF across multiple metrics, requiring lower average QP solving time, lower control effort, and substantially fewer control-design parameters, while improving both speed and path tracking (see Table 1 for statistics).

Acknowledgements

This research was supported by the Bundesministerium für Digitales und Verkehr (German Federal Ministry for Digital and Transport) within the project “Harmonizing Mobility” (grant number 19FS2035A).

References

- [1] Ayush Agrawal and Koushil Sreenath. Discrete control barrier functions for safety-critical control of discrete systems with application to bipedal robot navigation. In *Robotics: Science and Systems XIII*. Robotics: Science and Systems Foundation, 2017.
- [2] Aaron D. Ames, Samuel Coogan, Magnus Egerstedt, Gennaro Notomista, Koushil Sreenath, and Paulo Tabuada. Control barrier functions: Theory and applications. In *2019 18th European Control Conference (ECC)*, pages 3420–3431, Naples, Italy, 2019. IEEE.
- [3] Aaron D. Ames, Jessy W. Grizzle, and Paulo Tabuada. Control barrier function based quadratic programs with application to adaptive cruise control. In *53rd IEEE Conference on Decision and Control*, pages 6271–6278, 2014.
- [4] Aaron D. Ames, Xiangru Xu, Jessy W. Grizzle, and Paulo Tabuada. Control barrier function based quadratic programs for safety critical systems. *IEEE Transactions on Automatic Control*, 62(8):3861–3876, 2017.
- [5] Stephen P. Boyd and Lieven Vandenberghe. *Convex Optimization*. Cambridge University Press, Cambridge, UK ; New York, 2004.
- [6] Bolun Dai, Rooholla Khorrambakht, Prashanth Krishnamurthy, Vinícius Gonçalves, Anthony Tzes, and Farshad Khorrami. Safe navigation and obstacle avoidance using differentiable optimization based control barrier functions. *IEEE Robotics and Automation Letters*, 8(9):5376–5383, 2023.

- [7] Steven Diamond and Stephen Boyd. CVXPY: A Python-embedded modeling language for convex optimization. *Journal of Machine Learning Research*, 17(83):1–5, 2016.
- [8] Desong Du, Shaohang Han, Naiming Qi, Haitham Bou Ammar, Jun Wang, and Wei Pan. Reinforcement learning for safe robot control using control lyapunov barrier functions. In *2023 IEEE International Conference on Robotics and Automation (ICRA)*, pages 9442–9448, London, United Kingdom, 2023. IEEE.
- [9] Shao-Chen Hsu, Xiangru Xu, and Aaron D. Ames. Control barrier function based quadratic programs with application to bipedal robotic walking. In *2015 American Control Conference (ACC)*, pages 4542–4548, 2015.
- [10] Mrdjan Jankovic. Robust control barrier functions for constrained stabilization of nonlinear systems. *Automatica*, 96:359–367, 2018.
- [11] Taekyung Kim, Robin Inho Kee, and Dimitra Panagou. Learning to refine input constrained control barrier functions via uncertainty-aware online parameter adaptation. In *2025 IEEE International Conference on Robotics and Automation (ICRA)*, *in Press*, 2025.
- [12] Hengbo Ma, Bike Zhang, Masayoshi Tomizuka, and Koushil Sreenath. Learning differentiable safety-critical control using control barrier functions for generalization to novel environments. In *2022 European Control Conference (ECC)*, pages 1301–1308, 2022.
- [13] S. Monaco and D. Normand-Cyrot. Minimum-phase nonlinear discrete-time systems and feedback stabilization. In *26th IEEE Conference on Decision and Control*, volume 26, pages 979–986, 1987.
- [14] Quan Nguyen and Koushil Sreenath. Exponential control barrier functions for enforcing high relative-degree safety-critical constraints. In *2016 American Control Conference (ACC)*, pages 322–328, Boston, MA, USA, 2016. IEEE.
- [15] Xiao Tan, Ersin Daş, Aaron D. Ames, and Joel W. Burdick. Zero-order control barrier functions for sampled-data systems with state and input dependent safety constraints. In *2025 American Control Conference (ACC)*, pages 283–290, 2025.
- [16] Wei Xiao and Calin Belta. High-order control barrier functions. *IEEE Transactions on Automatic Control*, 67(7):3655–3662, 2022.
- [17] Wei Xiao, Calin Belta, and Christos G. Cassandras. Adaptive control barrier functions. *IEEE Transactions on Automatic Control*, 67(5):2267–2281, 2022.
- [18] Yuhang Xiong, Di-Hua Zhai, Mahdi Tavakoli, and Yuanqing Xia. Discrete-time control barrier function: High-order case and adaptive case. *IEEE Transactions on Cybernetics*, 53(5):3231–3239, 2023.
- [19] Jianye Xu and Bassam Alrifae. A learning-based control barrier function for car-like robots: Toward less conservative collision avoidance. In *2025 European Control Conference (ECC)*, pages 988–995. IEEE, 2025.
- [20] Jianye Xu, Chang Che, and Bassam Alrifae. A real-time control barrier function-based safety filter for motion planning with arbitrary road boundary constraints. In *2025 IEEE 28th International Conference on Intelligent Transportation Systems (ITSC)*, *in Press*, 2025.

A Computing Control-Design Parameters

We explain how we compute the reported numbers of control-design parameters for aTTCBF, PACBF, and

RACBF in Table 1. We define the total number of control-design parameters as

$$n_{\text{design}} := n_w + n_{\mathcal{K}}, \quad (\text{A.1})$$

where n_w and $n_{\mathcal{K}}$ count tunable weighting coefficients in the QP cost and tunable parameters of class \mathcal{K} functions that are introduced by the specific CBF method, respectively. We do not count tunable parameters shared across all methods (for example, weights used to penalize deviation from the same nominal controller).

In corridor navigation, there are $n_{\text{obs}} = 16$ obstacles and two corridor boundaries, hence the number of safety constraints is $n_{\text{safe}} = 2 + n_{\text{obs}} = 18$. Each safety constraint has relative degree $r = 2$. Each class \mathcal{K} function carries one scalar tunable parameter.

Our aTTCBF introduces one adaptive gain per safety constraint, with each having one associated weight in the QP cost. No other class- \mathcal{K} parameters are tuned because the class \mathcal{K} function is coefficient-free. Therefore, applying (A.1) with $n_w = n_{\text{safe}}$ and $n_{\mathcal{K}} = 0$ yields

$$n_{\text{design}} = 18 + 0 = 18. \quad (\text{A.2})$$

PACBF introduces $(r - 1)$ auxiliary penalty dynamics per safety constraint. Each such auxiliary component contributes (i) one QP weight (for its associated virtual input and/or relaxation term in the method-specific cost) and (ii) one class- \mathcal{K} parameter through the method-specific stabilization/safety inequalities. This yields the method-level counts $n_w = 2n_{\text{safe}}(r - 1)$ and $n_{\mathcal{K}} = 2n_{\text{safe}}(r - 1)$. With $n_{\text{safe}} = 18$ and $r = 2$,

$$n_{\text{design}} = 2 \cdot 18(2 - 1) + 2 \cdot 18(2 - 1) = 36 + 36 = 72. \quad (\text{A.3})$$

RACBF introduces, per safety constraint, (i) two method-specific QP weights and (ii) two coupled HOCBF chains (one for h and one for the adaptive relaxation), plus one additional class- \mathcal{K} parameter from the method-specific CLF term used to regulate the relaxation. This gives $n_w = 2n_{\text{safe}}$ and $n_{\mathcal{K}} = n_{\text{safe}}(2r + 1)$, yielding

$$n_{\text{design}} = 2 \cdot 18 + 18(2 \cdot 2 + 1) = 36 + 90 = 126. \quad (\text{A.4})$$